Efficient Image Sharpness Assessment Based on Content Aware Total Variation

Khosro Bahrami, *Student Member, IEEE*, and Alex C. Kot, *Fellow, IEEE*

***Abstract*—State-of-the-art sharpness assessment methods are mostly based on edge width, gradient, high-frequency energy, or pixel intensity variation. Such methods consider very little the image content variation in conjunction with the sharpness assessment which causes the sharpness metric to be less effective for different content images. In this paper, we propose an efficient no-reference image sharpness assessment called content aware total variation (CATV) by considering the importance of image content variation in sharpness measurement. By parameterizing the image TV statistics using generalized Gaussian distribution, the sharpness measure is identified by the standard deviation, and the image content variation evaluator is indicated by the shape parameter. However, the standard deviation is content-dependent which is different for the regions with strong edges, high frequency textures, low frequency textures, and blank areas. By incorporating the shape-parameter in moderating of the standard deviation, we propose a content aware sharpness metric. The experimental results show that the proposed method is highly correlated with the human vision system and has better sharpness assessment results than the state-of-the-art techniques on the blurred subset images of LIVE, TID2008, CSIQ, and IVC databases. Also, our method has very low computational complexity which is suitable for online applications. The correlations with the subjective of the four databases and statistical significance analysis reveal that our method has superior results when compared with previous techniques.**

***Index Terms*—Content aware total variation (CATV), human vision system (HVS), image sharpness/blurriness assessment.**

I. Introduction

ASSESSMENT of image quality has an important role in the modern multimedia applications, which can be done by human vision, but it is time consuming and is not practical. Therefore, development of methods for objective quality assessment is necessary for today's multimedia systems.

In the last few years, different approaches have been proposed for Image Quality Assessment (IQA) which are classified into three categories, namely full-reference (FR) [1]–[4], reduced-reference (RR) [5]–[10] and no-reference (NR) [11]–[36]. In the FR approaches [1]–[4], the reference image is available and the similarity between the distorted image and the reference image is measured. In the RR approaches [5]–[10], partial information from the image is used for quality assessment. However, in the practical applications, the reference image does not exist, so the FR and RR approaches can not be used. In such cases, NR-IQA approaches [11]–[36] are applicable. In this paper, we focus on NR assessment of image sharpness/blurriness.

A lot of sharpness assessment methods have been proposed in the literature [11]–[36] and details are described in Section II. Most of these methods use various features such as edge width, gradient, high-frequency energy or pixel intensity variations. However, these methods have problem in accurate sharpness evaluation of the different content images. For instance, for two images with the same sharpness but different content variation, if the first one has strong edges and high-frequency textures, while the second one has blank (saturated) areas and mid-frequency textures, the existing methods detect the first image sharper than the second image due to the higher content variation. The reason is that the existing methods do not consider the image content variation together with the sharpness information in sharpness evaluation.

For instance, if the edge width or pixel intensity variation is used as a metric for sharpness assessment, the different content variations, e.g., texture and edges, highly affect the measured sharpness. There is similar weakness for the methods based on the gradient. For instance, texture and edges have different gradients which result the gradient based methods measure different values for the images with the same sharpness and different content variations. The methods based on high-frequency energy have the same weakness. Since the edges and textures have various high-frequency energy, these methods may generate different sharpness values for the images with the same sharpness and different content variations. As an example, consider two sharp images taken from the reference images of LIVE database [43] shown in Fig. 1(a) and (e). These two images are different in terms of content variation. The first one has lots of strong edges and high-frequency textures, while the second one has blank (saturated) areas and mid-frequency textures. The two sharp images (a) and (e) are being blurred with Gaussian blur with standard deviation of (b) and (f) 0.4; (c) and (g) 0.7; and (d) and (h) 0.9. So, the sharpness is the same for (a) and (e); (b) and (f); (c) and (g); (d) and (h), while the sharpness is decreased from (a) to (d) and from (e) to (h). The sharpness value of the images are calculated by the state-of-the-art methods including LPC-SI [25], S3 [16], blind/referenceless image spatial quality evaluator (BRISQUE) [18], BLIINDS-II [29], and ARISM [36], shown in Fig. 1(a)–(h), after scaling the scores into [0 1] on LIVE database. Smaller value means less sharpness.

The weakness of the state-of-the-art methods is that, the calculated sharpness values by these methods do not accurately indicate the actual sharpness value of the images with different

Manuscript received November 12, 2015; revised February 10, 2016 and May 15, 2016; accepted May 15, 2016. Date of publication May 25, 2016; date of current version July 15, 2016. The associate editor coordinating the review of this manuscript and approving it for publication was Dr. Xiaokang Yang.

The authors are with the School of Electrical and Electronic Engineering, Nanyang Technological University, Singapore 639798 (e-mail: khosro1@ntu.edu.sg; eackot@ntu.edu.sg).

Color versions of one or more of the figures in this paper are available online at http://ieeexplore.ieee.org.

Digital Object Identifier 10.1109/TMM.2016.2573139

Fig. 1. Example to the weakness of the state-of-the-art methods. The two sharp images, (a) and (e), are being blurred with Gaussian blur with the standard deviation of (b) and (f): 0.4; (c) and (g): 0.7; and (d) and (h): 0.9. Sharpness is decreasing from (a) to (d) and (e) to (h) while each image pair [(a) and from (e); (b) and (f); (c) and (g); (d) and (h)] has the same sharpness/blurriness. The measured sharpness values by LPC-SI [25], S3 [16], BRISQUE [18], BLIINDS-II [29], and ARISM [36] are not consistent with the actual sharpness values of the corresponding images, as highlighted in bold.

content, as highlighted in colour bold. For instance, the calculated sharpness of the images (b) and (e) by LPC-SI are 0.9848 and 0.9688, respectively, while the image (e) is sharper than (b). This is due to lower content variation of the image (e) than (b), which results in a less accurate sharpness score. The calculated sharpness value of the images (b) and (e) by S3 are 0.8936 and 0.8447, respectively, but the image (e) is actually sharper than (b). Similar cases can be observed for images (d) and (g) using BRISQUE; for the images (b) and (e) using BLIINDS-II; and for the images (b) and (e) using ARISM. Such observations show that these existing methods cannot detect the sharpness of the different content images accurately. This motivates us to propose a new sharpness metric which measures the sharpness of different contents images correctly.

In this paper, we address this drawback by proposing a content aware sharpness assessment metric. Following the prior works on content aware blur analysis [37], and sharpness assessment based on the image total variation (TV) [16], we studied the statistics of image TV. We found that the TV can also be used for content variation measurement. For instance, a smooth region such as sky has a smaller TV than a region with strong edges, and a high-contrast region exhibits a larger TV than a low-contrast region. Since the TV is affected by the content variation as well as the sharpness, we propose a content aware sharpness measure to address the weakness of the previous methods in sharpness measurement of different content images.

We extracted two features from the TV distribution to measure the sharpness and the content variation. Then, we propose a sharpness metric using such features to measure the sharpness of the different content images accurately and we name this as content aware total variation (CATV). The sharpness indicates the width of the TV distribution while the content variation changes the shape of TV distribution which varies from Gaussian to hyper-laplacian. Since the generalized Gaussian distribution (GGD) is a general family of Gaussian and hyper-laplacian distributions, these statistics revealed that by parameterizing the image TV with GGD, the standard deviation provides information about the sharpness and the shape-parameter provides content variation information. By incorporating both content variation as well as sharpness features, we develop a content aware sharpness metric called CATV. Our method has the following contributions. First, the objective score generated by our method is content aware and highly correlated with the subjective sharpness score reported by the existing public available databases. Second, we will show that our method has better sharpness assessment results than the state-of-the-art methods. Third, since the proposed features are calculated in the spatial domain, our method has low computational complexity which is suitable for online applications. Therefore, our method is efficient in terms of correlation with the subjective, improvement compared to the state-of-the-art methods and computational time.

The rest of this paper is organized as follows. A brief review of the related works are presented in Section II. In Section III, we introduce our proposed method for NR image sharpness assessment. Experimental results and discussions are given in Section IV. Section V concludes the paper.

II. Related Works

Various methods have been proposed to measure the image sharpness in the literature. We categorize the prior works into spatial-domain, transform-domain and gradient-domain categories. In what follows, we review these methods in details.

A. Spatial-Domain

In the spatial-domain category, we consider the image content such as the edge width and texture variation. Marziliano *et al.* [11] proposed a method to measure the sharpness by averaging the edge width along horizontal and vertical directions. Ferzli *et al.* [12] proposed the just noticeable blur (JNB) concept, which is a blur detection probability model based on the human vision. By incorporating the JNB, Narvekar *et al.* [13] introduced the cumulative probability of blur detection (CPBD) based on the human blur perception at different contrasts.

In addition to the edge-based approaches discussed, some other approaches used image pixels intensity variation. Vu *et al.* [16] proposed a sharpness measure named S3 by incorporating the image TV in the spatial domain and the image local spectral information. We proposed earlier in [17] a fast sharpness measure named MLV by calculating the maximum local variation of each pixel with respect to its 8-neighbors. Mittal *et al.* [18] introduced the BRISQUE by employing the statistics of locally luminance values to quantify the image quality. In another work, Mittal *et al.* [19] proposed a blind IQA model that only makes use of measurable deviations from statistical regularities observed in natural images, called natural image quality evaluator.

B. Transform-Domain

The transform-domain category examines the image in the discrete cosine, fourier and wavelet transform domain. The sharpness measurement techniques proposed in this category are motivated by the fact that reducing the sharpness decreases the image high frequency energy. In [22], Shaked *et al.* utilized the high and low frequency information, considering the issue that the image details indicated by the high frequency can be used as the sharpness measure. Janez *et al.* [23] measured the sharpness by calculating the discrete cosine transform (DCT) of the local image patches. Caviedes *et al.* [24] proposed a sharpness measure by combining the kurtosis of DCT coefficient distribution and the edge information. Hassen *et al.* [25] introduced a sharpness metric by incorporating local phase coherence (LPC) at the image spatial locations.

There are other approaches which measure the image sharpness based on the statistics of transform coefficients. Moorthy *et al.* [26], [27] proposed a NR-IQA model named Distortion Identification-based Image INtegrity and Verity Evaluation (DIIVINE) by utilizing the natural scene statistics of wavelet coefficients. Saad *et al.* [28], [29] proposed the complementary methods in [26], [27] called BLind Image Notator using DCT Statistics (BLIINDS) based on the statistics of DCT coefficients. In [30], Shen *et al.* introduced a hybrid of cosine, curvelet and wavelet transform for sharpness assessment. Gu *et al.* [36] proposed a new NR blind sharpness metric in the autoregressive parameter space, dubbed as AR-based image sharpness metric (ARISM).

C. Gradient-Domain

The gradient-domain category which employs the image gradient is motivated by the observation that the amplitude of gradient is reduced by decreasing the sharpness. In [31], Zhu *et al.* proposed a sharpness metric based on singular value decomposition applied to the local patches gradient. Ong *et al.* [32] used the average extend of edges in both directions of the gradient to determine the image sharpness. Chung *et al.* [33] proposed a method by incorporating the standard deviation and weighted mean of the edge gradient magnitude for sharpness measurement.

The drawback of these methods in all three categories is that they are less directly related to the content. Also, it should be mentioned that in addition to the accuracy, computational time is important in sharpness assessment for real-time applications. Such an objective is another issue which motivates us to work in spatial domain. In this paper, we demonstrate that a combination of two measures, sharpness and image content variation, yields to an effective measure of perceived sharpness well suited for online applications.

III. Proposed Method

The proposed method is summarized as follows. The input image is partitioned into blocks and the TV of the blocks are calculated to generate an overall image TV map. We model the TV statistics by GGD to extract the standard deviation used as the sharpness indicator and the shape-parameter utilized as an evaluator for the content variation. By moderating the standard deviation using the shape-parameter, we propose a content aware sharpness measure. The following sections provide detailed steps of the proposed method.

A. TV Map Composition

In this section, we generate the TV map of the input image $\mathbf{I}$. Let $\mathbf{I}$ be a color image of size $M \times N$, we convert it to the gray scale image $\mathbf{G}$, and then partition $\mathbf{G}$ into blocks $\mathbf{G}_{i,j}$ with $L \times L$ pixels, where *i* and *j* are index for different blocks ($1 \leq i \leq \lfloor \frac{M}{L} \rfloor$, $1 \leq j \leq \lfloor \frac{N}{L} \rfloor$). Similar to [16], we calculate below the TV of each block $\mathbf{G}_{i,j}$, denoted as $\Psi_g(\mathbf{G}_{i,j})$

$$\Psi_g(\mathbf{G}_{i,j}) = \{\max(\psi(\mathbf{P}_{m,n}))|1 \leq m < L, 1 \leq n < L\} \quad (1)$$

where

$$\psi(\mathbf{P}_{m,n}) = \sum_{m'=m}^{m+1} \sum_{n'=n}^{n+1} ||P(m,n) - P(m',n')|| \quad (2)$$

is the TV of the 2×2 block $\mathbf{P}_{m,n}$, at location (m,n) ($1 \leq m < L, 1 \leq n < L$) in $\mathbf{G}_{i,j}$, and $P(m,n)$ and $P(m',n')$ are the pixels at locations (m,n) and (m',n') in $\mathbf{G}_{i,j}$, respectively. $||.||$ denotes l_1 norm. For $\mathbf{P}_{m,n}$, we choose the smallest block size (block size of 2×2) to capture all the variations (vertical, horizontal and diagonal) in the smallest local region. In this case, we can calculate the sharpest value in the smallest region in each block $\mathbf{G}_{i,j}$ which is well correlated by the human vision system (HVS) [16].

The TV of all image blocks $\mathbf{G}_{i,j}$, $\Psi_g(\mathbf{G}_{i,j})$, are used to generate the TV of the whole image $\mathbf{G}$, denoted as $\Psi_g(\mathbf{G})$,

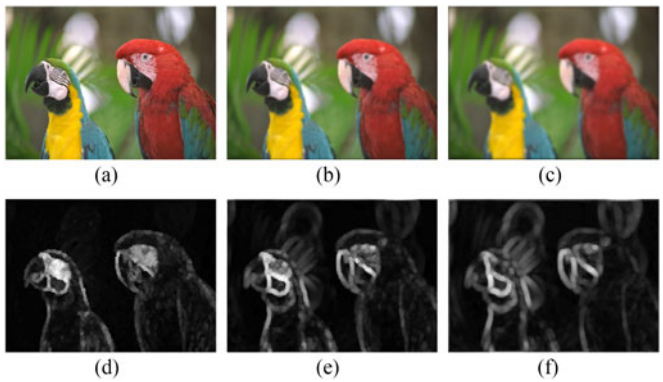

Fig. 2. TV map for three images with different sharpness. (a)–(c) include a reference image and the blurred versions from LIVE database by increasing the blurriness from (a) to (c). (d)–(f) show the TV maps.

where

$$\Psi_g(\mathbf{G}) = \begin{pmatrix} \Psi_g(\mathbf{G}_{1,1}) & \cdots & \Psi_g(\mathbf{G}_{1,\lfloor \frac{N}{L} \rfloor}) \\ \vdots & \ddots & \vdots \\ \Psi_g(\mathbf{G}_{\lfloor \frac{M}{L} \rfloor,1}) & \cdots & \Psi_g(\mathbf{G}_{\lfloor \frac{M}{L} \rfloor,\lfloor \frac{N}{L} \rfloor}) \end{pmatrix}. \quad (3)$$

Fig. 2(a)–(c) show three images from LIVE database by increasing the blurriness from (a) to (c) and their corresponding TV maps generated by our method in (d)–(f), respectively. The TV maps of the images with different sharpness show different brightness and sharpness for the edges and textures. For sharper images, the TV maps show brighter values for the edges and textures. Also, the edges look sharper and narrower and textures show more details. In contrast, in the TV maps of the images with more blurriness, the edges look wider with gray color and the textures look smoother.

In the literature, some methods [39]–[41] extended the traditional TV to Vectorial Total Variation (VTV), also called color TV, by considering the TV of RGB color channels. For RGB color images, the variations within color channels is more correlated with human vision. If one channel has higher variation than the other, the variation can be captured by using VTV between two channels as well as within the same channel. We extend the grayscale TV calculated in (1) to color TV to capture the highest content variation in the three RGB channels as follows.

For a given color image $\mathbf{I}$, we partition $\mathbf{I}$ into blocks $\mathbf{I}_{i,j}$ with $L \times L$ pixels, where i and j are the index of the blocks ($1 \le i \le \lfloor \frac{M}{L} \rfloor, 1 \le j \le \lfloor \frac{N}{L} \rfloor$). We calculate $\Psi_c(\mathbf{I}_{i,j})$, the VTV of the color blocks $\mathbf{I}_{i,j}$, below by extending (1) for three RGB color channels to yield

$$\Psi_c(\mathbf{I}_{i,j}) = \max\{\psi(\mathbf{Q}_{m,n,r}) | 1 \le m < L, 1 \le n < L, r = 1,2,3\} \quad (4)$$

where $\psi(\mathbf{Q}_{m,n,r})$ is the TV of all 2×2 overlapping blocks $\mathbf{Q}_{m,n,r}$ with color channel r ($r = \{1,2,3\}$) at location (m,n) in $\mathbf{I}_{i,j}$. We calculate $\psi(\mathbf{Q}_{m,n,r})$ using (2) for each color channel. Afterward, the VTV of the image blocks $\mathbf{I}_{i,j}$ are used to generate the VTV of the image $\mathbf{I}$, denoted as $\Psi_c(\mathbf{I})$.

For an input color image, we can use either TV and VTV to calculate the sharpness measure for gray scale and color space, respectively. In the next section, we explain our proposed method based on TV, while by replacing TV with VTV we consider three RGB color channels.

B. Sharpness and Content Variation Features Extraction

Using the pixels value in the TV map of the image $\mathbf{G}$, we generate the TV distribution. We extract two features from the distribution of TV, as the sharpness measure and content variation evaluator. The TV distribution of the low-frequency textures and blank areas is different from the TV distribution of the high-frequency textures and strong edges. In addition, the TV distribution is affected by the sharpness, meaning that by decreasing the sharpness, the variance of the TV is reduced. Such observation suggests that a general model can be used to parameterize the TV distribution of the image. We parameterize below the TV statistics with the GGD, the general form of Gaussian, laplacian and hyper-laplacian distributions, also used in IQA methods to parameterize natural scene statistic of the image [17], [26], [29]

$$f(\Psi_g(\mathbf{G});\mu,\gamma,\sigma) = \left(\frac{\gamma}{2\sigma\Gamma(\frac{1}{\gamma})\sqrt{\frac{\Gamma(\frac{1}{\gamma})}{\Gamma(\frac{3}{\gamma})}}} \right) e^{-\left(\frac{|\Psi_g(\mathbf{G})-\mu|}{\sigma\sqrt{\frac{\Gamma(\frac{1}{\gamma})}{\Gamma(\frac{3}{\gamma})}}} \right)^{\gamma}} \quad (5)$$

where $\Psi_g(\mathbf{G})$ is the TV of the gray scale image $\mathbf{G}$, $\Gamma(.)$ is the gamma function obtained using the method in [42], μ is the mean, σ is the standard deviation and γ ($\gamma > 0$) is the shape-parameter of the GGD. In (5), we can use $\Psi_c(.)$ instead of $\Psi_g(.)$ to parameterize the statistics of VTV.

By modeling the TV statistics using GGD, the standard deviation σ can be used as a sharpness measure metric which is reduced by decreasing the sharpness. As an example, consider three sharp images selected from the reference images of LIVE database [43], shown in Fig. 3(a), (d) and (g), we blur these three images with Gaussian blur kernel with standard deviation of 3 and 6, shown in Fig. 3(b), (e), (h), and Fig. 3(c), (f), (i), respectively. The TV distribution of these images together with the calculated σ of the TV distribution are shown in Fig. 3. We can observe that by increasing the blurriness in an image, the TV distribution becomes narrower, showing that the standard deviation σ is decreased.

However, for the images of the same sharpness but with different content variations, e.g., images (a), (d) and (g), the estimated σ varies which results in affecting the accuracy of the sharpness measurement. To get better insight, consider the three images (a), (g) and (h) in Fig. 3. Since the images (a) and (g) are taken from the reference images of LIVE database, they have the same sharpness while the images (g) and (h) have the same content with different sharpness. By estimating σ value for these three images, we observe that the difference of σ for (a) and (h) is smaller than (a) and (g) due to the lower content variation in (a) compare to (g). In such case, σ is highly affected by the image content, resulted in the calculated sharpness of image (a) to be much smaller than (g). To overcome this problem, we take into account γ extracted from the GGD of TV as a content evaluator to moderate σ as a content aware sharpness measure.

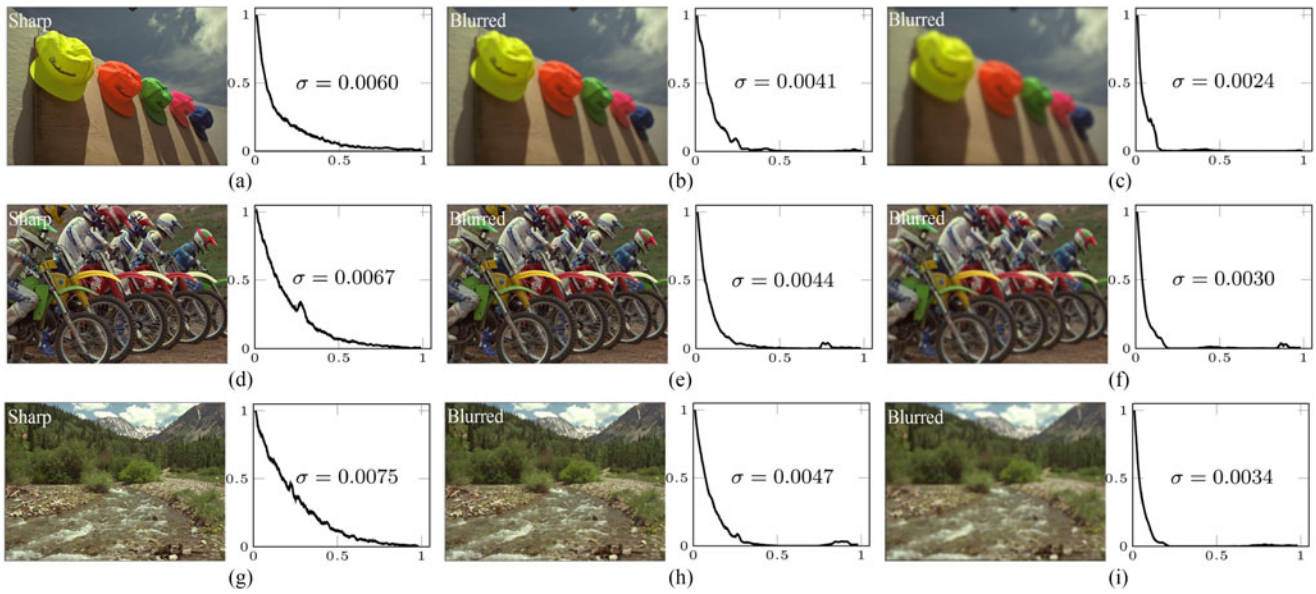

Fig. 3. Three sets of examples to show the level of blurriness versus the TV distributions of the images. (a), (d), and (g) are three sharp images selected from the reference images of, LIVE database. (b), (e), and (h) are the blurred versions of (a), (d), and (g), respectively, when blurred with a Gaussian blur kernel with standard deviation of 3. (c), (f), and (i) are the blurred versions of (a), (d), and (g), respectively, when blurred with a Gaussian blur kernel with standard deviation of 6. By increasing the blurriness in the images (from left to right), the TV distribution becomes narrow and σ of the TV distribution is decreased. For TV distributions, the X axis indicates the normalized TV values into the range [0, 1] which is divided by the histogram bins. The Y axis indicates how many values fall in each bin of the TV histogram, which is normalized between 0 and 1.

Following our study on the TV statistics, the GGD of TV of natural images can vary from hyper-laplacian to Gaussian ($0 < \gamma \leq 2$) due to the image content variation. The γ close to 0 indicates that the image has a low content variation, while γ close to 2 reveals that the image has a high content variation, meaning that γ can be used as a content variation evaluator. For the sharp images shown in Fig. 3, the estimated γ of the images are (a) $\gamma = 0.4170$, (d) $\gamma = 0.8060$ and (g) $\gamma = 1.1720$, showing the increment of the image content variation.

We define the images with $0 < \gamma \leq 1$ as low content variation and the images with $1 < \gamma \leq 2$ as high content variation. The images whose shape-parameter exhibits a value in $0 < \gamma \leq 1$ have more blank regions and low-frequency textures, whereas the images with $1 < \gamma \leq 2$ include more high-frequency textures and strong edges. In the next section, we propose the sharpness metric by utilizing σ and γ.

C. Content Aware Sharpness Assessment Feature

By incorporating the standard deviation σ and the shape-parameter γ of the GGD of image TV as sharpness measure and content variation evaluator, respectively, we use γ as a weight to moderate σ. For low content variation images ($\gamma \leq 1$), we use γ to magnify σ while for high content variation images ($1 < \gamma$) we utilize γ to reduce σ. As such, we use the inverse of γ, $\frac{1}{\gamma}$, to define the moderated sharpness measure as

$$\Upsilon(\sigma, \gamma) = \frac{\sigma}{\gamma} \tag{6}$$

such that for low content variations images, $\frac{1}{\gamma}$ ($\frac{1}{\gamma} \geq 1$) increases the sharpness measure from σ to $\frac{\sigma}{\gamma}$ while for high content variations images, $\frac{1}{\gamma}$ ($\frac{1}{\gamma} < 1$) decreases the sharpness measure from σ to $\frac{\sigma}{\gamma}$. Therefore, by taking into account γ, the TV distribution is changed in such a way that it makes the sharpness metric be content aware.

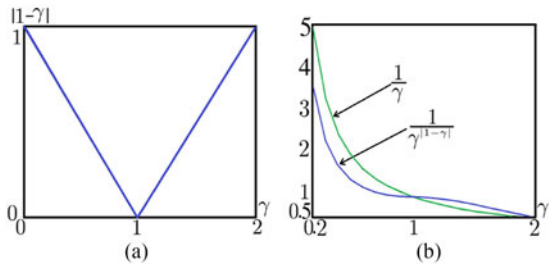

Fig. 4. (a) Curve of $|1-\gamma|$ for $0 < \gamma < 2$. (b) Curves of $\frac{1}{\gamma}$ and $\frac{1}{\gamma^{|1-\gamma|}}$.

Instead of γ, we introduce here $\gamma^{|1-\gamma|}$. The reason is that, when the content variation of the image is not very low or very high (γ close to 1), we don't want to moderate the value of σ with γ, while when the content variation of the image is low (γ close to 0) or high (γ close to 2), we want to moderate the value of σ with γ. With these conditions, we propose $\frac{1}{\gamma^{|1-\gamma|}}$ instead of $\frac{1}{\gamma}$ which fits our needs. In such case, when γ is close to 1, $|1-\gamma|$ ($|1-\gamma|$ is close to 0) as the power of γ reduces the impact of γ in moderating σ, while when γ is close to 0 or 2, $|1-\gamma|$ ($|1-\gamma|$ is close to 1) as the power of γ increases the impact of γ in moderating σ. Fig. 4(a) shows the curve of $|1-\gamma|$ for $0 < \gamma < 2$.

Fig. 4(b) shows the curves of $\frac{1}{\gamma}$ and $\frac{1}{\gamma^{|1-\gamma|}}$ when γ is varying in the range of $[0.22]$. When $\gamma = 1$, the slope of $\frac{1}{\gamma^{|1-\gamma|}}$ is zero. By increasing the value of γ to 2 or decreasing it to 0, the slope of $\frac{1}{\gamma^{|1-\gamma|}}$ is increased. This means that when the γ is close to 0 or 2, $\frac{1}{\gamma^{|1-\gamma|}}$ has more tendency to change the σ compare to when the γ is close to 1.

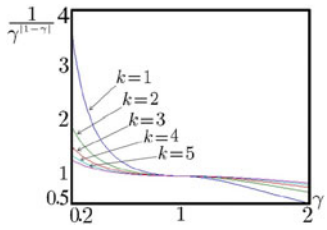

Fig. 5. Curve of $\frac{1}{\gamma^{\frac{|1-\gamma|}{k}}}$ for $k = 1, 2, 3, 4, 5$.

TABLE I
STUDY ON THE VALUE OF k USING CC AND SROCC CRITERIA ON THE BLURRED IMAGES OF LIVE AND TID2008 DATABASES

	LIVE database [43]			TID2008 database [44]	
k	CC	SROCC	k	CC	SROCC
1	0.9595	0.9513	1	0.8901	0.9235
2	**0.9632**	**0.9635**	**2**	**0.9113**	**0.9128**
3	0.9636	0.9619	3	0.9000	0.9047
4	0.9635	0.9619	4	0.8978	0.8990
5	0.9632	0.9609	5	0.8942	0.8978

By utilizing an integer parameter $k \in \{1, 2, 3, \ldots\}$ as the scaling factor of $|1-\gamma|$, we can tune the value of $|1-\gamma|$ to be more effective. By increasing k from 1, we can achieve an effective sharpness measure. Derived from (6), we define the tunable moderated sharpness measure as

$$\Upsilon(\sigma, \gamma, k) = \frac{\sigma}{\gamma^{\frac{|1-\gamma|}{k}}} \tag{7}$$

where σ is the standard deviation, γ is the shape-parameter, and k is the scaling factor chosen empirically.

Fig. 5 shows the curve of $\frac{1}{\gamma^{\frac{|1-\gamma|}{k}}}$ for $k = 1, 2, \ldots, 5$ when γ is varying in the range of [0.2-2]. For $\gamma > 1$ (high content variation images), the value of $\frac{1}{\gamma^{\frac{|1-\gamma|}{k}}}$ decreases the sharpness measure while for $\gamma < 1$ (low content variation images), $\frac{1}{\gamma^{\frac{|1-\gamma|}{k}}}$ increases the sharpness measure. The ratio of increment and decrement depends on the value of k. By increasing k, the ratio is reduced and the maximum ratio is achieved for $k = 1$. Also, by increasing k, the slope of curve is decreased, implying that $\frac{1}{\gamma^{\frac{|1-\gamma|}{k}}}$ has less impact on moderating σ.

We study on the value of k to achieve a reasonably good performance highly correlated with the HVS. The value of two criteria including pearson Correlation Coefficient (CC) and Spearman Rank-Order Correlation Coefficient (SROCC) for LIVE [43] and TID2008 [44] public databases for $k = 1, \ldots, 5$ are shown in Table I. The best CC and SROCC for LIVE and TID2008 databases are achieved for $k = 2$. By selecting $k = 2$, which results in a high correlation with HVS, our proposed sharpness measurement metric is written as

$$\Upsilon(\sigma, \gamma) = \frac{\sigma}{\gamma^{\frac{|1-\gamma|}{2}}}. \tag{8}$$

TABLE II
COMPARISON OF OUR PROPOSED METHOD AND PREVIOUS WORKS ON THE BLURRED IMAGES OF LIVE, TID2008, CSIQ, AND IVC DATABASES

LIVE database [43]					
Method	**CC**	**SROCC**	**RMSE**	**MAE**	**OR**
JNB [12]	0.8390	0.8368	11.8365	9.3485	0.2471
CBPD [13]	0.9107	0.9437	8.9857	6.8869	0.1609
DIIVINE [26]	Used LIVE for training				
BLIINDS-II [29]	Used LIVE for training				
BRISQUE [18]	Used LIVE for training				
S3 [16]	0.9537	**0.9645**	8.1235	5.1320	0.1090
LPC-SI [25]	0.9204	0.9594	8.5061	6.8987	0.1522
MLV [17]	0.9590	0.9566	6.1676	4.8928	0.0517
ARISM [36]	0.9560	0.9511	6.1676	4.8928	0.0517
Proposed (TV)	**0.9632**	0.9635	**5.8459**	**4.7618**	**0.0460**
Proposed (VTV)	**0.9659**	**0.9661**	**5.6322**	**4.4994**	**0.0402**
TID2008 database [44]					
Method	**CC**	**SROCC**	**RMSE**	**MAE**	**OR**
JNB [12]	0.7171	0.7045	0.8081	0.6254	0.7033
CBPD [13]	0.8316	0.8406	0.6438	0.5019	0.6500
DIIVINE [26]	0.8429	0.8322	0.6655	0.5031	0.6302
BLIINDS-II [29]	0.8415	0.8387	0.6339	0.4010	**0.5200**
BRISQUE [18]	0.8044	0.7989	0.6972	0.5059	0.6200
S3 [16]	0.8492	0.8327	0.6195	0.4790	0.6200
LPC-SI [25]	0.8574	0.8531	0.6040	0.4856	0.6800
MLV [17]	0.8585	0.8548	0.6018	0.4675	0.6100
ARISM [36]	0.8544	0.8681	0.6098	0.4675	0.6100
Proposed (TV)	**0.9113**	**0.9128**	**0.4833**	**0.3884**	0.5800
Proposed (VTV)	**0.9131**	**0.9202**	**0.4785**	**0.3763**	**0.5500**
CSIQ database [45]					
Method	**CC**	**SROCC**	**RMSE**	**MAE**	**OR**
JNB [12]	0.8060	0.7620	0.1696	0.1393	0.3670
CBPD [13]	0.8820	0.8860	0.1349	0.1245	0.3730
DIIVINE [26]	0.8912	0.8930	0.1132	0.0951	0.2653
BLIINDS-II [29]	0.9102	0.8915	0.1187	0.0943	0.2867
BRISQUE [18]	0.9274	0.9025	0.1072	0.0822	0.2400
S3 [16]	0.9035	0.9017	0.1228	0.0996	0.3400
LPC-SI [25]	0.9061	0.9071	0.1151	0.0927	0.2733
MLV [17]	0.9069	0.9247	0.1069	0.0749	0.1933
ARISM [36]	0.9481	0.9255	0.0911	0.0749	0.2170
Proposed (TV)	**0.9548**	**0.9334**	**0.0851**	**0.0680**	**0.1933**
Proposed (VTV)	**0.9627**	**0.9453**	**0.0776**	**0.0605**	**0.1467**
IVC database [46]					
Method	**CC**	**SROCC**	**RMSE**	**MAE**	
JNB [12]	0.7992	0.7722	0.8609	0.6374	
CBPD [13]	0.8865	0.8404	0.6629	0.5126	
DIIVINE [26]	0.8012	0.7984	0.5767	0.4325	
BLIINDS-II [29]	0.7837	0.5312	0.5893	0.4444	
BRISQUE [18]	0.8515	0.8239	0.4510	0.3775	
S3 [16]	0.9333	0.8916	0.4099	0.3266	
LPC-SI [25]	0.9726	0.9398	0.2653	0.2017	
MLV [17]	0.9812	0.9767	0.2203	0.1514	
ARISM [36]	0.9780	0.9544	0.2203	0.1514	
Proposed (TV)	**0.9855**	**0.9819**	**0.1936**	**0.1392**	
Proposed (VTV)	**0.9843**	**0.9819**	**0.2012**	**0.1583**	

IV. EXPERIMENTAL RESULTS AND DISCUSSION

In this section, we compare the performance of our method with the state-of-the-art methods like JNB [12], CPBD [13], DIIVINE [26], BLIINDS-II [29], BRISQUE [18], S3 [16], LPC-SI [25], MLV [17], and ARISM [36] for sharpness assessment of the blurred images of LIVE [43], TID2008 [44], CSIQ [45] and IVC [46] databases.

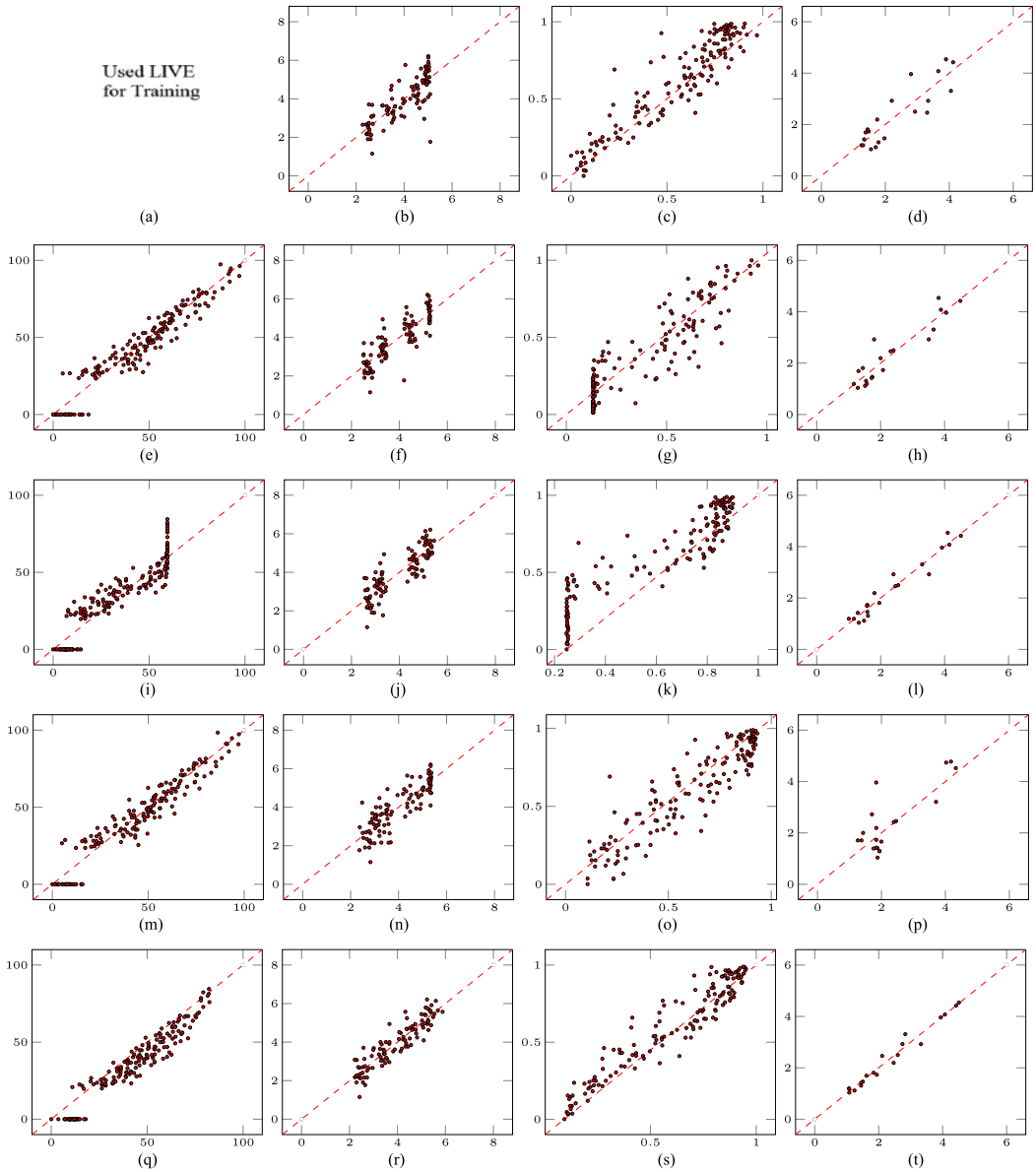

Fig. 6. Scatter plots of the subjective sharpness scores generated by BLIINDS-II, BRISUQE, S3, LPC-SI, ARISM, and our method versus the objective sharpness scores reported by the blurred images of LIVE, TID2008, CSIQ, and IVC after nonlinear mapping. (a) BRISQUE, LIVE. (b) BRISQUE, TID2008. (c) BRISQUE, CSIQ. (d) BRISQUE, IVC. (e) S3, LIVE. (f) S3, TID2008. (g) S3, CSIQ. (h) S3, IVC. (i) LPC-SI, LIVE. (j) LPC-SI, TID2008. (k) LPC-SI, CSIQ. (l) LPC-SI, IVC. (m) ARISM, LIVE. (n) ARISM, TID2008. (o) ARISM, CSIQ. (p) ARISM, IVC. (q) Proposed method, LIVE. (r) Proposed method, TID2008. (s) Proposed method, CSIQ. (t) Proposed method, IVC.

A. *Experimental Setup*

To setup the experiment, the reference and blurred images of four public available databases are utilized including LIVE [43], TID2008 [44], CSIQ [45] and IVC [46]. The LIVE, TID2008, CSIQ and IVC have 174, 100, 150 and 20 images, respectively. The range of scores in LIVE, TID2008, CSIQ and IVC are [0 100], [0 8], [0 1] and [0 6], respectively. In LIVE and CSIQ, the subjective scores are reported as the different of mean opinion scores (DMOS), while in TID2008 and IVC, the subjective scores are reported as mean opinion scores (MOS) [47]. Five criteria are used to compare the performance of different methods including pearson Correlation Coefficient (CC), Spearman Rank-Order Correlation Coefficient (SROCC), Root Mean Square Error (RMSE), Mean Absolute Error (MAE) and Outlier Ratio (OR) which are carried out by the video quality experts group (VQEG) [47].

B. *Statistical Comparison With NR Methods*

We compare the performance of our method, with JNB [12], CPBD [13], DIIVINE [26], BLIINDS-II [29], BRISQUE [18], S3 [16], LPC-SI [25], MLV [17], and ARISM [36] for sharpness assessment, in terms of CC, SROCC, RMSE, MAE and OR criteria, in Table II. We evaluate our method by considering the statistics of TV and VTV. In TV, the images are converted to grayscale to generate the TV statistics, while in VTV, the three RGB color channels of the images are used. For each criteria, the top two best results are highlighted with boldface. For all

TABLE III
EVALUATION OF OUR PROPOSED METHOD IN SHARPNESS MEASUREMENT OF DIFFERENT CONTENT IMAGES IN FIG. 1

First image			
(a) Sharp	**(b) Blurred s.d. = 0.4**	**(c) Blurred s.d. = 0.7**	**(d) Blurred s.d. = 0.9**
0.9950	0.7573	0.6770	0.5397
Second image			
(e) Sharp	**(f) Blurred s.d. = 0.4**	**(g) Blurred s.d. = 0.7**	**(h) Blurred s.d. = 0.9**
0.9704	0.6954	0.6217	0.4912

databases, our proposed method dominates and achieves the best overall performance for sharpness assessment.

C. Scatter Plots of Subjective Versus Objective Scores

Fig. 6 shows the scatter plots of the objective sharpness scores generated by BRISUQE, S3, LPC-SI, ARISM and our method versus the subjective sharpness scores reported by the blurred subset images of LIVE, TID2008, CSIQ and IVC databases after nonlinear mapping. Our method shows less biasness in subjective versus objective sharpness scoring when compared with the previous techniques. For instance, the scatter plot of our technique for CSIQ database in Fig. 6(w) shows a better spread along the diagonal line.

D. Sharpness Assessment of Different Content Images

In this experiment, we evaluate our proposed method in sharpness measurement of different content images, shown in Fig. 1. As stated in the Section I, the weakness of the state-of-the-art methods is that they are less accurate in sharpness assessment of different content images.

We show the calculated sharpness value of the two images and their blurred versions in Table III. The calculated sharpness values by our proposed method show more accurate sharpness measurement than the previous works in Fig. 1. From left to right, by decreasing the sharpness of the images, the sharpness value by our method is decreasing which is consistent for the same and different content images.

E. Statistical Significant Analysis

In the statistical significance analysis, a variance-based hypothesis test on the residual difference between the subjective sharpness scores and the objective sharpness scores is conducted. This analysis uses F-statistic to analyze the variance of residuals distributions while assumes that the residuals follow a Gaussian distribution. The test is based on the ratio of variances of residuals of two methods to determine whether the two residual sets come from the same distribution [1]. Table IV shows the standard deviation of the residual between objective sharpness scores generated by different methods and subjective sharpness scores reported by the blurred images of four databases. Smaller standard deviation reveals lower variation between the subjective and objective score. In this experiment, we use the statistics of TV. The result shows that our method has the lowest variance for all four databases.

TABLE IV
STANDARD DEVIATIONS OF THE RESIDUALS BETWEEN OBJECTIVE SHARPNESS SCORES GENERATED BY DIFFERENT METHODS AND THE SUBJECTIVE SHARPNESS SCORES REPORTED BY THE BLURRED IMAGES OF LIVE, TID2008, CSIQ, AND IVC DATABASES

Method	LIVE	TID2008	CSIQ	IVC
JNB [12]	12.0376	11.6438	16.7931	14.7370
CBPD [13]	11.5145	10.1782	14.0140	12.2913
DIIVINE [26]	-	12.3635	11.9642	14.0756
BLIINDS-II [29]	-	23.0867	8.2484	21.7722
BRISQUE [18]	-	12.7463	7.5765	8.9486
S3 [16]	9.9077	11.2668	9.4359	7.6615
LPC-SI [25]	11.8360	11.5090	12.2252	5.0442
ARISM [36]	8.4634	15.4264	7.4575	6.3633
Proposed (TV)	**6.1353**	**9.1629**	**6.0378**	**4.0823**

To compare the inferiority or superiority of the methods based on the residuals variance test, a statistical significance analysis matrix is created, shown in Table V. Each entry of the table consists of combinations of four symbols 1, 0, x, and -. The label entries using these symbols in arranged according to LIVE, TID2008, CSIQ and IVC databases. The symbol 1 indicates that the method in the row is statistically better than the one in the same column, 0 denotes that the method in the column is better than the one in the same row, x indicates that the two methods are statistically indistinguishable, and the symbol - indicates that the database has not been used for variance analysis of the method. Most label entries in the last row contain 1, which shows our method is statistically superior to the previous methods for the blurred images of these four databases.

F. Local Sharpness Map

In this section, we show the ability of our proposed metric in local sharpness map generation. Although, we calculate the sharpness metric for the assessment of image quality at the global level, by applying the proposed method in block wise fashion, local sharpness map can also be computed. To generate the local sharpness map, we use the image blocks $G_{i,j}$ of size 4×4 ($L = 4$) to compute the TV. We consider a patch around each blocks $G_{i,j}$ with size of 8×8 to parameterize the local sharpness with GGD. Our sharpness map is composed using the sharpness value for each block $G_{i,j}$. Fig. 7(a)–(d) show four images from LIVE database by increasing the blurriness from (a) to (d) and their corresponding sharpness maps generated by our method in (e)–(h), respectively.

Although the sharpness value of the whole image can also be calculated based on the block based version of our method, it does not have better performance than the global based version of our method. The reason is that, in the block based version of our method, the sharpness value of the whole image is calculated by taking the average of all local sharpness values. Therefore, the regions which are less important in the sharpness measurement based on HVS, e.g. regions without any content, affect the calculated sharpness value. Table VI shows the performance of the block-based version of our method by considering different block sizes for LIVE database. The result shows that, the global

TABLE V
STATISTICAL SIGNIFICANCE ANALYSIS MATRIX CREATED BASED ON THE RESIDUALS BETWEEN THE OBJECTIVE SHARPNESS SCORES GENERATED BY THE SHARPNESS METHODS AND THE SUBJECTIVE SHARPNESS SCORE REPORTED USING THE BLURRED IMAGES OF LIVE, TID2008, CSIQ, AND IVC DATABASES

Method	JNB	CPBD	DIIVINE	BLIINDS-II	BRISQUE	S3	LPC-SI	ARISM	Proposed
JNB [12]	x x x x	0 0 0 x	− x 0 x	− 0 1 x	− x 1 x	0 0 0 0	0 0 0 0	0 0 0 0	0 0 0 0
CPBD [13]	1 1 1 x	x x x x	− x 0 1	− 1 0 1	− 1 0 x	0 1 0 0	x x x 0	x x x 0	0 x 0 0
DIIVINE [26]	− x 1 x	− x x x	− x x x	− 1 0 1	− x x 0	− x x 0	− x x 0	x x x 0	− 0 0 0
BLIINDS-II [29]	− 1 0 x	− 0 1 0	− 0 1 0	− x x x	− 0 x 0	− 0 x 0	− 0 1 0	− 0 1 0	− 0 0 0
BRISQUE [18]	− x 0 x	− 0 1 x	− x x 1	− 1 x 1	− x x x	− x 1 x	− 0 1 0	− 0 1 0	− 0 x 0
S3 [16]	1 1 1 1	1 0 1 1	− x x 1	− 1 x 1	− x 0 x	x x x x	1 x 1 x	1 x 1 x	0 x 0 x
LPC-SI [25]	1 1 1 1	x x x 1	− x x 1	− 1 0 1	− x 0 1	0 x 0 x	x x x x	x x x x	0 x 0 x
ARISM [36]	1 1 1 1	x x x 1	− x x 1	− 1 0 1	− x 0 1	0 x 0 x	x x x x	x x x x	0 x x x
Proposed	1 1 1 1	1 x 1 1	− 1 1 1	− 1 1 1	− 1 x 1	1 x 1 x	x x x x	1 x x x	x x x x

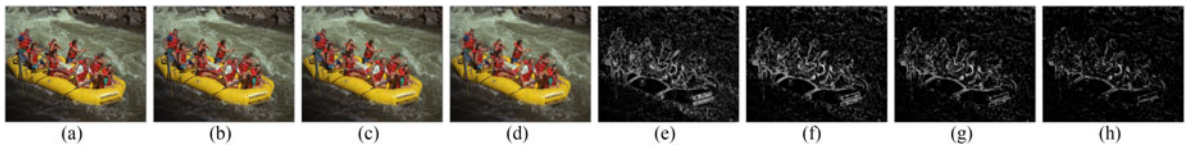

Fig. 7. Sharpness map of the proposed method. (a)–(d) include a reference image and the blurred versions from the LIVE database. (e)–(h) show the sharpness maps generated by the proposed method.

TABLE VI
COMPARISON OF CC, SROCC, AND RMSE OF THE BLOCK BASED VERSION OF OUR METHOD FOR SHARPNESS ASSESSMENT OF THE BLURRED IMAGES OF LIVE DATABASE BY CONSIDERING DIFFERENT BLOCK SIZES

Block Size ($L \times L$)	CC	SROCC	RMSE
4×4	0.9588	0.9574	6.0352
8×8	0.9601	0.9595	5.9535
16×16	0.9603	0.9606	5.9894
32×32	0.9598	0.9602	6.0154

TABLE VII
COMPARISON OF MEAN COMPUTATIONAL TIME OF METHODS IN GENERATING SHARPNESS SCORE OF 200 IMAGES WITH SIZE OF 3264×2448

Method	S3 [16]	DIVINE [29]	BRISQE [26]	LPC [25]	MLV [17]	ARISM [36]	Proposed
Time (sec)	367.6	470.2	**2.3**	19.5	**1.6**	35.4	**4.2**

TABLE VIII
COMPARISON OF CC, SROCC, RMSE AND THE COMPUTATIONAL TIME OF OUR METHOD ON THE BLURRED IMAGES OF LIVE DATABASE BY CONSIDERING OVERLAPPING AND NON-OVERLAPPING SCHEMES FOR DIFFERENT BLOCK SIZES

Block Size ($L \times L$)	Overlapping (d)	CC	SROCC	RMSE	Time (seconds)
4×4	0	0.9602	0.9607	6.1324	62.8
4×4	2	0.9603	0.9610	6.0666	204.2
8×8	0	0.9622	0.9620	5.8439	48.7
8×8	2	0.9622	0.9618	5.8768	533.2
8×8	4	0.9624	0.9626	5.8781	148.1
16×16	**0**	**0.9632**	**0.9635**	**5.8459**	**44.6**
16×16	4	0.9628	0.9626	5.8770	491.4
16×16	8	0.9628	0.9627	5.8775	135.3
32×32	0	0.9630	0.9631	5.8573	47.9
32×32	8	0.9628	0.9626	5.8770	488.2
32×32	16	0.9628	0.9626	5.8773	498.5

sharpness measure which was reported in the Table II with CC=0.9632, SROCC=0.9635, and RMSE=5.8459 has better results compare to the block-based sharpness for different block sizes.

G. Computational Complexity Analysis

Since our method works in spatial domain without complex mathematical operation or transformation, the computational complexity is low. The main computational cost of our technique is determined by the computation of TV/VTV of each pixel which is linear with respect to the number of pixels.

We compare the mean runtime of seven sharpness measurement methods applied to 200 images with size 3264×2448 from Google web site. This test is performed on a PC with Intel Core i5 CPU at 3.20 GHz, 8GB RAM, Windows 7 64-bit, and Matlab 7.11. Table VII shows the mean runtime of the images for different methods. Our method with TV statistics is slower than MLV and BRISQUE but faster than the remaining five methods.

H. Overlapping Versus Non-overlapping Strategy

In this section, we evaluate overlapping and non-overlapping strategies in partitioning of $\mathbf{G}$ into blocks $\mathbf{G}_{i,j}$ for sharpness assessment. We measure the performance of the proposed method for different block sizes ($L = 4, 8, 16, 32$) and overlapping pixels d ($d = 0, 2, 4, 6$ where $d = 0$ refers to non-overlapping case). We show the performance of our method for the blurred images of LIVE database based on four criteria including CC, SROCC, RMSE and Time (the required time to process all the images), in Table VIII. The results show that, in general, the overlapping strategy does not have better performance than non-overlapping strategy while having higher computational time. Among different block sizes, we select non-overlapping scheme with block size of 16×16 ($L = 16$) for the experimental results.

I. The Effect of Noise

Here, we discuss the effect of white Gaussian noise on the sharpness measure of our method. In terms of image sharpness,

Fig. 8. (a) and (b) are two reference images from the LIVE database. (c) and (d) are the images when contaminated with Gaussian noise.

the previous sharpness measurement techniques [16], [25] reported that adding noise may increase [16] or decrease [25] the sharpness of an image. The evaluation of our proposed method reveals that by adding noise, the perceived sharpness is reduced and the amount of reduction depends on the image content variation which is consistent with the perception of HVS.

Based on the HVS, the impact of noise on the image sharpness is content dependent. For instance, adding noise to a region with strong edges or high frequency textures may decrease the perceived sharpness of the region a little, because it is hard for the HVS to see the details in the image. In contrast, adding noise to a smooth region or low frequency textures may decrease the perceived sharpness of the image a lot. Therefore, perceived sharpness of the noisy image by HVS can not be easily predicted which is affected by the content variation of the image [16], [25].

Fig. 8 shows (a) an image with low content variation and (b) an image with high content variation. The computed sharpness of the images by our methods are (a) 0.94 and (b) 0.96. By adding Gaussian noise to these images, we generate the noisy images (c) and (d). The sharpness value of the noisy images are (c) 0.82 and (d) 0.87. The result shows that the sharpness value of the image with low content variations drops more than the image with high content variations, which is consistent with the perception of HVS.

We measure the sharpness value of the images in Fig. 8 by the sharpness measurement techniques [16], [25]. The computed sharpness of the images by the method [16] are (a) 0.83 and (b) 0.88 while the sharpness value of the noisy images are (c) 0.90 and (d) 0.96. It shows that adding noise increase the sharpness value of the images which may not be consistent with the HVS. The computed sharpness of the images by the method [25] are (a) 0.88 and (b) 0.93. By adding Gaussian noise to these images, measured sharpness value of the noisy images drop to (c) 0.82 and (d) 0.83. The result shows that the sharpness value of the image with low content variations does not drop more than the image with high content variations, which is not consistent with the perception of HVS.

V. Conclusion

In this paper, a novel technique was proposed for image sharpness assessment based on CATV. By extracting two features (standard deviation and shape-parameter) from GGD of the image TV, the former is used to measure sharpness while the later is incorporated to evaluate image content variation. Since sharpness of the images is affected by the content, shape-parameter is utilized to moderate the standard deviation as a content aware sharpness measure. Using such a metric, we are able to quantify the sharpness of the same content and different content images more accurate than the previous methods. The experimental results show that the proposed method, highly correlated with HVS in terms of sharpness, has better sharpness assessment results than the state-of-the-art methods for the blurred subset images of four commonly used databases, namely LIVE, TID2008, CSIQ and IVC. Further, our method was evaluated using scatter plot of the objective versus subjective sharpness scores, significant analysis, computational complexity and sensitivity to noise. Based on various analysis and evaluations, our method has superior sharpness assessment results most of the times when compared to the state-of-the-art techniques.

One more applications of blur sharpness metric is to build a robust general-purpose NR-IQA framework as a component, as has been proposed in [48]. Since our proposed method is efficient in terms of correlation with the subjective, improvement compared to the state-of-the-art methods and computational time, it is suitable to be used as a component for real-time applications.

Acknowledgment

This work was carried out at the Rapid-Rich Object Search (ROSE) Laboratory at the Nanyang Technological University, Singapore. The ROSE Laboratory is supported by a grant from the Singapore National Research Foundation and administered by the Interactive and Digital Media Programme Office, Media Development Authority.

References

[1] R. Sheikh, M. F. Sabir, and A. C. Bovik, "A statistical evaluation of recent full reference image quality assessment algorithms," *IEEE Trans. Image Process.*, vol. 15, no. 11, pp. 3440–3451, Nov. 2006.

[2] R. Sheikh and A. C. Bovik, "Image information and visual quality," *IEEE Trans. Image Process.*, vol. 15, no. 2, pp. 430–444, Feb. 2006.

[3] Z. Wang, A. C. Bovik, H. R. Sheikh, and E. P. Simoncelli, "Image quality assessment: From error visibility to structural similarity," *IEEE Trans. Image Process.*, vol. 13, no. 4, pp. 600–612, Apr. 2004.

[4] C. Li and A. C. Bovik, "Content-partitioned structural similarity index for image quality assessment," *Signal Process. Image Commun.*, vol. 25, no. 7, pp. 517–526, 2010.

[5] L. Ma, S. Li, F. Zhang, and K. N. Ngan, "Reduced-reference image quality assessment using reorganized DCT-based image representation," *IEEE Trans. Multimedia*, vol. 13, no. 4, pp. 824–829, Aug. 2011.

[6] X. Gao, W. Lu, D. Tao, and X. Li, "Image quality assessment based on multiscale geometric analysis," *IEEE Trans. Image Process.*, vol. 18, no. 7, pp. 1409–1423, Jul. 2009.

[7] D. Tao, X. Li, W. Lu, and X. Gao, "Reduced-reference IQA in contourlet domain," *IEEE Trans. Syst., Man, Cybern.*, vol. 39, no. 6, pp. 1623–1627, Dec. 2009.

[8] R. Soundararajan and A. C. Bovik, "RRED indices: Reduced reference entropic differencing for image quality assessment," *IEEE Trans. Image Process.*, vol. 21, no. 2, pp. 517–526, Feb. 2011.

[9] K. Gu, G. Zhai, X. Yang, W. Zhang, "Automatic contrast enhancement technology with saliency preservation," *IEEE Trans. Circuits Syst. Video Technol.*, vol. 25, no. 9, pp. 1480–1494, Sep. 2015.

[10] K. Gu, G. Zhai, W. Lin, M. Liu, "The analysis of image contrast: from quality assessment to automatic enhancement," *IEEE Trans. Cybern.*, vol. 46, no. 1, pp. 284–297, Jan. 2015.

[11] P. Marziliano, F. Dufaux, S. Winkler, and T. Ebrahimi, "A no-reference perceptual blur metric," in *Proc. Int. Conf. Image Process.*, 2002, vol. 3, pp. III-57–III-60.

[12] R. Ferzli and L. Karam, "A no-reference objective image sharpness metric based on the notion of just noticeable blur (JNB)," *IEEE Trans. Image Process.*, vol. 18, no. 4, pp. 717–728, Apr. 2009.

[13] N. Narvekar and L. Karam, "A no-reference image blur metric based on the cumulative probability of blur detection (CPBD)," *IEEE Trans. Image Process.*, no. 99, pp. 2678–2683, Sep. 2011.

[14] J. Caviedes and S. Gurbuz, "No-reference sharpness metric based on local edge kurtosis," in *Proc. Int. Conf. Image Process.*, Sep. 2002, vol. 3, pp. III-53-III-56.
[15] S. Varadarajan and L. J. Karam, "An improved perception-based noreference objective image sharpness metric using iterative edge refinement," in *Proc. 15th IEEE Int. Conf. Image Process.*, Oct. 2008, pp. 401–404.
[16] C. Vu, T. Phan, and D. Chandler, "S3: A spectral and spatial measure of local perceived sharpness in natural images," *IEEE Trans. Image Process.*, vol. 21, no. 3, pp. 934–945, Mar. 2012.
[17] K. Bahrami and A. C. Kot, "A fast approach for no-reference image sharpness assessment based on maximum local variation," *IEEE Signal Process. Lett.*, vol. 21, no. 6, pp. 751–755, Jun. 2014.
[18] A. Mittal, A. Moorthy, and A. Bovik, "No-reference image quality assessment in the spatial domain," *IEEE Trans. Image Process.*, vol. 21, no. 12, pp. 4695–4708, Dec. 2012.
[19] A. Mittal, R. Soundararajan, and A. C. Bovik, "Making a completely blind image quality analyzer," *IEEE Signal Process. Lett.*, vol. 20, no. 3, pp. 209–212, Mar. 2013.
[20] S. Zhong, Y. Liu, Y. Liu, and F. Chung, "A semantic no-reference image sharpness metric based on top-down and bottom-up saliency map modeling," in *Proc. IEEE Int. Conf. Image Process.*, Sep. 2010, pp. 1553–1556.
[21] L. He, D. Tao, X. Li, and X. Gao, "Sparse representation for blind image quality assessment" in *Proc. IEEE Conf. Comput. Vis. Pattern Recog.*, Jun. 2012, pp. 1146–1153.
[22] D. Shaked and I. Tastl, "Sharpness measure: Towards automatic image enhancement," in *Proc. IEEE Int. Conf. Image Process.*, Sep. 2005, vol 1, pp. I-937–I-940.
[23] M. K. Janez and S. Kovacic, "A Bayes-spectral-entropy-basedmeasure of camera focus using a discrete cosine transform," *Pattern Recog. Lett.*, vol. 27, no. 13, pp. 1431–1439, 2006.
[24] J. Caviedes and F. Oberti, "A new sharpness metric based on local kurtosis, edge and energy information," *Signal Process. Image Commun.*, vol. 19, no. 2, pp. 147–161, 2004.
[25] R. Hassen, Z. Wang, and M. Salama, "Image sharpness assessment based on local phase coherence," *IEEE Trans. Image Process.*, vol. 22, no. 7, pp. 2798–2810, Jul. 2013.
[26] A. K. Moorthy and A. C. Bovik, "Blind image quality assessment: From natural scene statistics to perceptual quality," *IEEE Trans. Image Process.*, vol. 20, no. 12, pp. 3350–3364, Dec. 2011.
[27] A. K. Moorthy and A. C. Bovik, "A two-step framework for constructing blind image quality indices," *IEEE Signal Process. Lett.*, vol. 17, no. 5, pp. 513–516, May. 2010.
[28] M. Saad, A. Bovik, and C. Charrier, "DCT statistics model-based blind image quality assessment," in *Proc. IEEE Int. Conf. Image Process.*, Sep. 2011, pp. 3093–3096.
[29] M. Saad, A. Bovik, and C. Charrier, "Blind image quality assessment: A natural scene statistics approach in the DCT domain," *IEEE Trans. Image Process.*, vol. 21, no. 8, pp. 3339–3352, Aug. 2012.
[30] J. Shen, Q. Li, and G. Erlebacher, "Hybrid no-reference natural image quality assessment of noisy, blurry, JPEG2000, and JPEG images," *IEEE Trans. Image Process.*, vol. 20, no. 8, pp. 2089–2098, Aug. 2011.
[31] X. Zhu and P. Milanfar, "A no-reference sharpness metric sensitive to blur and noise,", in *Proc. Int. Workshop Quality Multimedia Experience*, 2009, pp. 64–69.
[32] E. Ong *et al.*, "A no-reference quality metric for measuring image blur," in *Proc. Int. Symp. Signal Process. Appl.*, vol. 1, 2003, pp. 469–472.
[33] Y. C. Chung, J. M. Wang, R. R. Bailey, S. W. Chen, and S. L. Chang, "A non-parametric blur measure based on edge analysis for image processing applications," in *Proc. IEEE Conf. Cybern. Intell. Syst.*,Dec. 2004, vol. 1, pp. 356–360.
[34] K. Gu, M. Liu, G. Zhai, X. Yang, W. Zhang, "Quality assessment considering viewing distance and image resolution," *IEEE Trans. Broadcast.*, vol. 61, no. 3, pp. 520–531, Sep. 2015.
[35] K. Gu *et al.*, "Content-weighted mean-squared error for quality assessment of compressed images," *Signal, Image Video Process.*, pp. 1–8, 2015.
[36] K. Gu, G. Zhai, W. Lin, X. Yang, and W. Zhang, "No-reference image sharpness assessment in autoregressive parameter space," *IEEE Trans. Image Process.*, vol. 21, no. 6, pp. 1–14, Oct. 2015.
[37] T. S. Cho *et al.*, "A content-aware image prior," in *Proc. IEEE Conf. Comput. Vis. Pattern Recog.*, Jun. 2010, 169-176..
[38] L. I. Rudin, S. Osher, and E. Fatemi, "Nonlinear total variation based noise removal algorithms," *Phys. D*, vol. 60, no. 14, pp. 259–268, 1992.
[39] P. Blomgren and T. F. Chan, "Color TV: Total variation methods for restoration of vector-valued images," *IEEE Trans. Image Process.*, vol. 7, no. 3, pp. 304–309, Mar. 1998.
[40] B. Goldluecke and D. Cremers, "An approach to vectorial total variation based on geometric measure theory," in *Proc. IEEE Conf. Comput. Vis. Pattern Recog.*, Jun. 2010, pp. 327–333.
[41] T. Miyata and Y. Sakai, "Vectorized total variation defined by weighted L infinity norm for utilizing inter channel dependency," in *Proc. IEEE Int. Conf. Image Process.*,Sep.-Oct. 2012, pp. 3057–3060.
[42] K. Sharifi and A. Leon-Garcia, "Estimation of shape parameter for generalized Gaussian distributions in subband decompositions of video," *IEEE Trans. Circuits Syst. Video Technol.*, vol. 5, no. 1, pp. 52–56, 1995.
[43] H. Sheikh, Z.Wang, L. Cormack, and A. Bovik, "LIVE image quality assessment database release 2," 2005. [Online]. Available: http://live.ece.utexas.edu/research/quality
[44] N. Ponomarenko *et al.*, "TID2008–a database for evaluation of full-reference visual quality assessment metrics," *Adv. Modern Radioelectron.*, vol. 10, no. 4, pp. 30–45, 2009.
[45] E. Larson and D. Chandler, "Most apparent distortion: Full-reference image quality assessment and the role of strategy," *J. Electron. Imag.*, vol. 19, no. 1, pp. 011006-1–011006-21, 2010.
[46] P. L. Callet and F. Autrusseau, "Subjective quality assessment IRCCYN/IVC database," 2005. [Online]. Available: http://www.irccyn.ec-nantes.fr/ivcdb/
[47] "Final report from the video quality experts group on the validation of objective models of video quality assessment," 2000. [Online]. Available: http://www.vqeg.org/
[48] K. Gu, G. Zhai, X. Yang, and W. Zhang, "Hybrid no-reference quality metric for singly and multiply distorted images," *IEEE Trans. Broadcast.*, vol. 60, no. 3, pp. 555–567, Sep. 2014.

Khosro Bahrami (S'11) received the B.Sc. degree in computer engineering from Shiraz University, Shiraz, Iran, in 2000, the M.Sc. degree in computer engineering from the Sharif University of Technology, Tehran, Iran, in 2002, and the Ph.D. degree in electrical and electronic engineering from Nanyang Technological University, Singapore, in 2015.

He is currently a Postdoctoral Researcher with the Biomedical Research Imaging Center, University of North Carolina, Chapel Hill, NC, USA. His research interests include computer vision, machine learning, deep learning, and medical imaging.

Dr. Bahrami served as a reviewer for the IEEE TRANSACTIONS ON IMAGE PROCESSING, the IEEE TRANSACTIONS ON MULTIMEDIA, the IEEE TRANSACTIONS ON SIGNAL PROCESSING, the IEEE TRANSACTIONS ON INFORMATION FORENSICS AND SECURITY, and the IEEE TRANSACTIONS ON CYBERNETICS.

Prof. Alex C. Kot (S'85-M'89-SM'98-F'06) has been with the Nanyang Technological University, Singapore, since 1991. He headed the Division of Information Engineering at the School of Electrical and Electronic Engineering for eight years and served as an Associate Chair (Research) and Vice Dean Research for the School of Electrical and Electronic Engineering. He is currently a Professor and Associate Dean for the College of Engineering, the Director of Rapid-Rich Object Search Laboratory, and the Director of the NTU-PKU Joint Research Institute. He has authored or coauthored works in the areas of signal processing for communication, biometrics, data-hiding, image forensics, information security, and image object retrieval and recognition.

Dr. Kot is a Fellow of IES and a Fellow of the Academy of Engineering, Singapore. He served as the Associate Editor for the IEEE TRANSACTIONS ON SIGNAL PROCESSING, the IEEE TRANSACTIONS ON MULTIMEDIA, the IEEE SIGNAL PROCESSING LETTERS, the *IEEE Signal Processing Magazine*, the IEEE JOURNAL OF THE SPECIAL TOPICS IN SIGNAL PROCESSING, the IEEE TRANSACTIONS ON CIRCUITS AND SYSTEMS FOR VIDEO TECHNOLOGY, the IEEE TRANSACTIONS ON INFORMATION, FORENSICS, AND SECURITY, the IEEE TRANSACTIONS ON IMAGE PROCESSING and the IEEE TRANSACTIONS ON CIRCUITS AND SYSTEMS PART II and PART I. He has served the IEEE Signal Processing Society in various capacities, such as the General Co-Chair for the 2004 IEEE International Conference on Image Processing and the Vice President for the IEEE Signal Processing Society. He was the recipient of the Best Teacher of the Year Award and is a co-author for several Best Paper Awards including ICPR, IEEE WIFS, and IWDW. He is the IEEE Distinguished Lecturer for the Signal Processing Society and the Circuits and Systems Society.